

Influence of machining conditions on the surface quality after circumferential milling of carbon fiber reinforced aluminum laminate

Elżbieta Doluk^{1*}, Marek Magdziak², Paweł Sułkowicz², Jarosław Buk²

¹ Department of Production Computerisation and Robotisation, Faculty of Mechanical Engineering, Lublin University of Technology, Nadbystrzycka 36, 20-618 Lublin, Poland

² Department of Manufacturing Techniques and Automation, Faculty of Mechanical Engineering and Aeronautics, Rzeszow University of Technology, al. Powstańców Warszawy 12, 35-959 Rzeszów, Poland

* Corresponding author's e-mail: e.doluk@pollub.pl

ABSTRACT

Fiber metal laminates (FMLs) are an increasingly used group of materials due to their properties. Thanks to their advantages, they are used in many areas of industry. An example of this type of material is carbon fiber reinforced aluminum laminate (CARALL). This paper presents the influence of machining conditions on surface quality and cutting forces after circumferential milling of a 3-layer CARALL. The workpieces were formed by combining two different materials: EN-AW 7075-T6 aluminium alloy and carbon fiber reinforced plastics (CFRP). The effects of cutting speed (v_c), feed rate (f_z) and helix angle (λ) on material height difference and feed force F_f were investigated. The experiment concluded that poorer surface quality and higher cutting forces were obtained for a tool with a higher helix angle. The parameters to obtain the best surface quality (the lowest material height difference) are cutting speed of 500 m/min, feed rate of 0.08 mm/tooth and helix angle of 20°. The lowest surface accuracy (the highest material height difference) was obtained after machining with the following parameters: cutting speed of 200 m/min, feed rate of 0.08 mm/tooth and helix angle of 35°.

Keywords: FMLs, milling, surface quality, cutting parameters, helix angle, feed force, CARALL.

INTRODUCTION

The constant development of technology forces the search for new engineering materials. Currently, composite materials and sandwich structures are very popular. To meet the new requirements for engineering materials, a new group of composite materials – fiber metal laminates (FMLs) – has been introduced. These materials belong to the family of structural composites, formed by combining thin layers of metals and polymer composites. The layers are joined by hot pressing and then cured, usually by vacuum impregnation. This combination results in materials with very good mechanical properties with the effect of reducing the weight of the construction [1]. Light metal alloys, such as aluminum, titanium and magnesium alloys, are usually used

as metal layers. As composite layers, fiber reinforced plastics (FRPs) such as carbon fiber reinforced plastics (CFRP), glass fiber reinforced plastics (GFRP) or aramid fiber reinforced plastics (AFRP) are usually applied [2].

FMLs are a group of structural materials that combine the properties of metals and plastics – high mechanical strength, impact resistance, ability to absorb vibration and sound, high stiffness, reduced weight, high fatigue resistance and resistance to cracking of the composite layer. Due to the above properties and the fact that these materials meet the tough conditions of the aviation industry, FMLs are often used for aircraft components (wings, skins, tails) [3, 4].

FMLs can be divided taking into account several subdivision criteria, for example using the criterion of metal materials used (e.g.

Aluminum-Based FMLs, Titanium-Based FMLs, Magnesium-Based FMLs), composite material reinforcement used (e.g. carbon-based FMLs, glass-based FMLs, aramid-based FMLs), lamination lay-up (e.g., 2/1 lay-up FMLs, 3/2 lay-up FMLs, 4/3 lay-up FMLs) and direction of the laminate (unidirectional hybrid laminates, cross ply hybrid laminates). In addition, aluminum-based FMLs can be divided into carbon fiber reinforced aluminum laminate (CARALL), glass fiber reinforced aluminum laminate (GLARE) and aramid fiber reinforced aluminum laminate (ARALL) [5, 6]. The main problem limiting the application of FMLs is the difficulty in machining them, mainly due to their anisotropy. High dimensional and form accuracy requirements in the aerospace industry require components with high surface quality and the absence of typical forms of damage to fiber composites, such as delamination, matrix burnout and fiber extraction [7, 8]. In addition, FMLs used in aircraft construction are often joined to form larger structures. If the deviations of the components are not correct, the joining process is hampered. The final stage in the production of such structures is to give them their final shape and dimensions, usually using milling or trimming processes. Many times protective and decorative coatings are applied to their surface. All this means that the quality of FML surfaces has a very strong influence on their further functioning, especially on the strength of the structure and its aesthetic qualities.

FMLs, like FRP and sandwich structures, are considered difficult materials to work with [9]. This is due to their non-uniform structure and highly abrasive components (the fiber reinforcing polymer composite). The machining of such materials is associated with rapid wear of cutting tools, the occurrence of forms of destruction of composite materials (delamination, matrix cracking and smearing, fiber pulling-out), injection of metal chips into the composite layer. This leads to the creation of a component with an accuracy not within the established deviations [10, 11]. Besides, machining FMLs containing aluminum alloys requires a balance between cutting speed and feed rate [12]. Therefore, it is very important to choose the right strategy for this type of materials.

A lot of academic papers focus on the effects of machining FMLs. However, the attention of the researchers has been mainly devoted to making holes and mounting connections in this type of material. In [13] a hole diameter, circularity

error and delamination at the entry zone of holes after drilling of CARALL composite were studied. The influence of technological parameters (cutting speed and feed rate) and the type of a tool (uncoated tool, TiAlN-coated tool and TiAl/TiAl-SiMoCr-coated tool) on the quality of holes was described. Based on the experiment, it was found that the uncoated drill produced a hole diameter that was closest to the nominal drill diameter. It was also noted that an increase in cutting speed resulted in an increase in circularity error, while an increase in feed rate led to greater delamination. They showed that the uncoated tool led to the least material delamination during machining. Mani et al. [14] described the effects of drill diameter, spindle speed and feed rate on cutting forces, delamination and hole surface roughness when drilling in FMLs reinforced with BaSo4 nanoparticles. They showed that among the considered machining conditions, the following parameters are the most suitable parameters for this type of material: spindle speed of 3000 rpm, feed rate of 10 mm/min and drill diameter of 6 mm. In [15], the effect of water-abrasive cutting parameters on the circularity, diameter of holes, surface roughness, types of damages and abrasive contamination after machining of GLARE was presented. They also proposed the E index (power of erosion) for selecting machining conditions for which there is no delamination of the machined material. They showed that the use of high water pressure makes it possible to obtain a hole with a diameter close to its nominal value of diameter. In addition, the distance of the cutting nozzle from the machined surface affects the shape of the hole – the use of a distance equal to 5 mm improves a cylindricity of a hole, but contributes to the undulation of its sidewalls. The processing parameters adopted in the experiment did not affect the roughness of hole surface, which confirmed that water-jet technology can be used as an alternative to the traditional drilling process.

Logesh et al. [16] presented the influence of drilling parameters (spindle speed, feed rate) and the type of matrix of the composite layer on the quality of holes made in GLARE. They showed that spindle speed had the greatest effect on the quality of the analysed material after processing. In [17], the results of a study of the ultrasonic-assisted drilling (UAD) process of CARALL are described. The paper presents the effects of machining parameters (spindle speed and feed rate), and ultrasonic amplitudes on the flexural

strength and the delamination factor. It was noted that among the processing conditions considered, the best results were obtained for the following values of parameter: spindle speed of 1500 rpm, feed rate of 0.05 mm/rev and ultrasonic amplitude of 10 μ m.

One alternative to traditional hole drilling in FMLs is helical milling [18]. Bolar et al. [19] compared the effects of drilling and helical milling of CARALL. Based on the results, they found that helical milling produced lower forces during machining. This process resulted in a better chip formation mechanism, which ultimately translated into better hole quality and less material delamination. A similar experiment was conducted by Wang et al. [20]. They compared hole quality after conventional drilling and helical milling of CFRP/Ti stacks. They showed that in addition to the optimal selection of machining parameters, an important issue is the control of cutting tool wear, which increases with the number of holes drilled, which directly affects the increase in cutting force.

The analysis of the literature presented reveals a lack of studies in the field of milling FMLs. Most of the available works refer to the properties of FMLs and their applicability [21–23]. Some researchers have focused on the accuracy of holes in parts made of this type of material, but there is currently no research on the effects of milling FMLs. Therefore, the purpose of this article is to evaluate the effectiveness of CARALL milling and to determine the influence of cutting speed, feed rate and tool geometry (helix angle) on the surface quality and cutting forces accompanying the process.

MATERIALS AND METHODS

The subjects of the experiment were 3-layer FMLs. The shape and dimensions of the tested samples are shown in Figure 1. The material considered consisted of 3 layers: two outer layers made of EN-AW-7075 (Al) aluminum alloy (ENAW-AlZn5.5MgCu) with a thickness of 0.3 mm, and an inner layer in the form of a CFRP with a thickness of 0.4 mm. The materials were chosen because of their frequent use in aviation [24].

EN-AW 7075-T6 aluminum alloy, whose chemical composition is shown in Table 1, is a material characterized by high mechanical strength, high hardness and high wear resistance, and low corrosion resistance. It is an alloy with high machinability and low weldability.

Due to its properties (Table 2), EN-AW 7075-T6 aluminum alloy has found use in applications requiring a combination of high hardness and strength while keeping the weight of the structure low. It is used in the aerospace industry (aircraft hardware, rocket parts), automotive industry

Table 2. Selected properties of EN-AW 7075-T6 [26]

| Property | Value |
|--------------------------------|-------|
| Density, g/cm ³ | 2.81 |
| Young's modulus (E), GPa | 71.7 |
| Thermal conductivity, W/m K | 155 |
| Hardness, HRC | 87 |
| Poisson's ratio (ν) | 0.32 |
| Ultimate tensile strength, MPa | 573 |
| Shear strength, MPa | 331 |
| Fatigue strength, MPa | 159 |

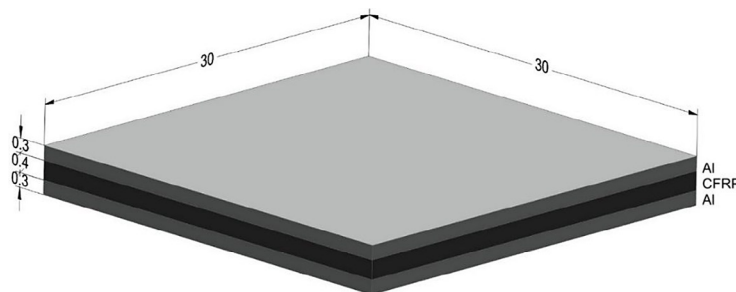


Figure 1. Shape and dimensions of the samples

Table 1. Chemical composition (%) of EN-AW 7075 [25]

| Al | Si | Fe | Cu | Mn | Mg | Cr | Zn | Ti | Other elements |
|-----------|------|------|---------|------|---------|-----------|---------|------|----------------|
| 87.1–91.4 | 0.40 | 0.50 | 1.2–2.0 | 0.30 | 2.1–2.9 | 0.18–0.28 | 5.1–6.1 | 0.20 | 0.15 |

(shafts, gears, bumpers), engineering industry (machine and equipment parts) or military industry (defence equipment).

The inner layer forming the FML was made of a CFRP in the form of a unidirectional T300 3K 40A C2 fabric from Toray company (Tokyo, Japan) with a fiber volume of 60%. A Hexply 913 modified epoxy resin with a low-temperature cure cycle from Hexcel company (Stamford, Connecticut, USA) was used as the matrix. The process of bonding the reinforcement and matrix was carried out at 125 °C for 60 minutes at a pressure of 0.7 MPa. As a result of this process, a structural prepreg with a thickness of 0.4 mm was obtained. Table 3 shows selected properties of the applied prepreg.

Prior to joining the materials, the aluminum layer was chromium-etched and roughened by hand using P320 grit sandpaper. The layers were bonded by pressure-vacuum impregnation using a resin as the matrix of the composite material. The process was carried out in an autoclave under the following conditions: temperature of 175 °C, pressure of 0.6 MPa, time of 120 min. The test materials were then subjected to a circumferential, down-milling process on a DMU 100 Mono-Block 5-axis machining centre from DMG MORI (Tokyo, Japan). To reduce the risk of delamination, the machining was carried out without the use of machining fluid. Figure 2 shows how the sample was clamped during machining.

The milling process was carried out with variable cutting parameters: cutting speed (v_c), feed rate (f_z), and with variable helix angle (λ). The experiment used a $3 \times 3 \times 2$ compound plan, by

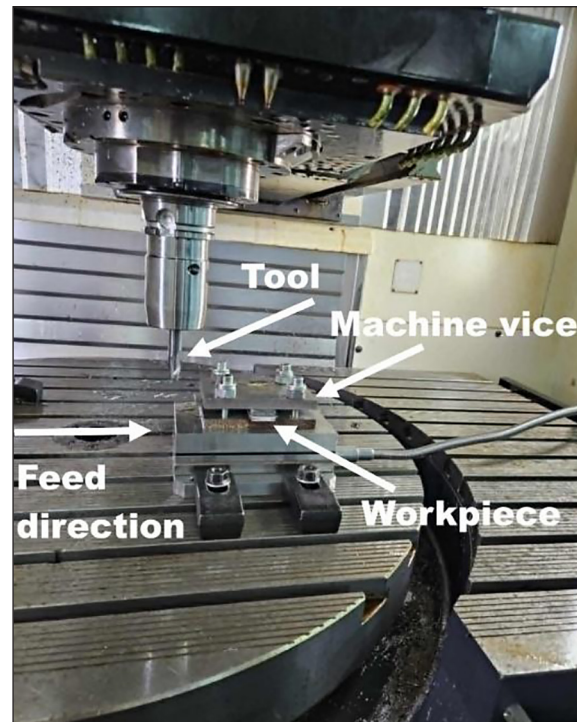


Figure 2. Machining set up

which the effect of 3 factors on the dependent variable was studied (Table 4). This plan was chosen as the best one to conduct preliminary research – in subsequent papers, the focus will be on implementing research according to the RSM.

The machining was carried out with a constant axial depth of cut (ADOC) of 2 mm and radial depth of cut (RDOC) of 0.5 mm. The values of the v_c and f_z parameters were selected taking into account the minimum, average and maximum values of the parameters recommended by the cutting tool manufacturer for milling aluminum alloys and polymer composites [27].

The applied tools were 2-blade, monolithic, uncoated milling cutters (Hoffman Group, Munich, Germany). The material of the milling cutters was fine-grained K10F carbide (90% WC, 10% Co). Two milling cutters of similar design were used, differing only in the helix angle (λ). The helix angle was taken as one of the independent variables, since it primarily affects the rate of

Table 3. Properties of the prepreg used

| Property | Value |
|---------------------------|-------|
| Tensile strength, MPa | 1.82 |
| Tensile modulus, GPa | 140 |
| Tensile Strain, % | 1.26 |
| Compressive strength, MPa | 1.47 |
| Flexural strength, MPa | 1.79 |
| Flexural modulus, GPa | 123 |
| ILSS, MPa | 94.10 |

Table 4. Plan of the experiment

| Factor | Level | | |
|---------------------------|---------------|---------------|---------------|
| Cutting speed (v_c) | 200 m/min | 350 m/min | 500 m/min |
| Feed rate (f_z) | 0.04 mm/tooth | 0.06 mm/tooth | 0.08 mm/tooth |
| Helix angle (λ) | 20° | | 35° |

chip removal, which directly affects the quality of the machined surface. Figure 3 shows the shape and dimensions of the used tools.

The experiment examined the surface quality of the samples and the cutting forces when cutting CARALL. The surface quality was determined by the material height difference, which is due to the different properties of the materials, mainly their machinability and stiffness. The material height difference therefore shows by what value one layer of the structure is offset relative to the adjacent layer. It was measured using an InfiniteFocus-Alicona optical instrument (Alicona Imaging GmbH, Graz, Austria). The material height differences occurring between the profile of the first aluminum alloy layer and the profile of the CFRP surface (ΔH_1) and the profile of the CFRP surface and the profile of the second aluminum alloy layer forming the test material (ΔH_2) were determined (Figure 4). The material height differences were defined on the basis of parallel straight lines

fitted to the profiles of the individual layers of the structure. The material height differences were determined, according to the equations:

$$\Delta H_1 = |H_{Al1} - H_{CFRP}| \quad (1)$$

$$\Delta H_2 = |H_{CFRP} - H_{Al2}| \quad (2)$$

where: ΔH_1 – material height difference between the first layer of the aluminum alloy and CFRP, ΔH_2 – material height difference between the CFRP and the second layer of aluminium alloy, H_{Al1} – line fitted to the profile of the first layer of the aluminum alloy, H_{CFRP} – line fitted to the profile of the CFRP, H_{Al2} – line fitted to the profile of the second layer of the aluminum alloy.

During the machining, cutting forces were also recorded using a piezoelectric multicomponent dynamometer for measuring the three orthogonal components of a cutting force (Kistler, Winterthur,

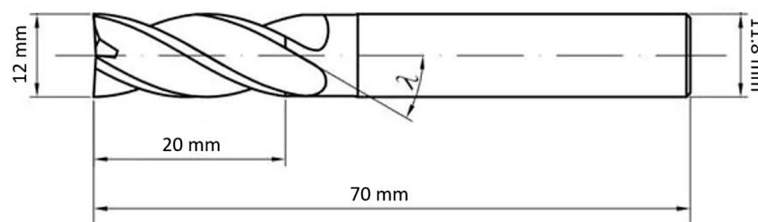


Figure 3. Shape and dimensions of the milling cutters used [27]

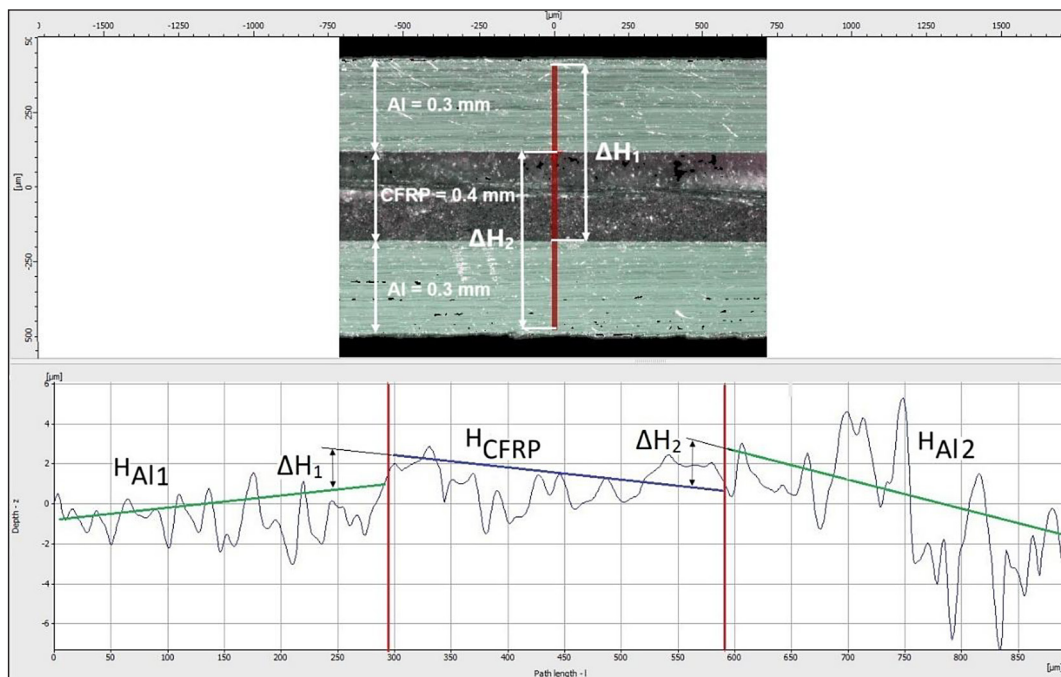


Figure 4. Material height difference

Switzerland). This device has a measuring range of up to 5 kN, and the signal is recorded at 3.5 kHz. The dynamometer was mounted on the table of the machining centre. A Kistler charge amplifier (type 5070A), which converted the measurement signal to electrical voltage, and a Kistler data acquisition system (DAQ) type 2825A-02 consisting of a data acquisition card and DynoWare software were also required to build a complete cutting force measurement system (Figure 5).

Measurements were made for the three components of the cutting force and then the results were analyzed. Based on a preliminary analysis, it was assessed that the highest values were obtained for the feed force (F_p), so it was further analyzed in Section 3. Figure 6 shows the test stand where the experiment was conducted.

The cutting process for each set of cutting parameters for both cutting tools was performed three times – the values of the studied variables were the average values of the measurements of the three samples.

RESULTS AND DISCUSSION

Material height difference

The material height differences were reported with an accuracy of 0.01 μm , which made it possible to better assess which machining conditions enabled a more accurate surface quality to be achieved after the milling process.

Figures 7–9 show the material height differences depending on the values of the v_c and f_z parameters for a tool with a helix angle of 20° .

For the f_z parameter of 0.04 mm/tooth, the highest value of the material height difference ($\Delta H_1 = 3.55 \mu\text{m}$) was obtained at a cutting speed of 350 m/min. In the case studied, the lowest value of the material height difference was achieved for ΔH_2 ($\Delta H_2 = 0.52 \mu\text{m}$) when the highest cutting speed was used ($v_c = 500 \text{ m/min}$). There was observed the same trend for ΔH_1 and ΔH_2 : the values of ΔH_1 and ΔH_2 increased and decreased for the same cutting speeds (Figure 7).






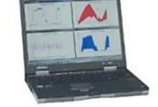
| | | | | | |
|---|---|---|---|--|---|
|  |  |  |  |  |  |
| Dynamometer | Connection cable | Charge amplifier | Connecting cable | DAQ system | PC with DynoWare |
| Type 9257B | Type 1687B5 | Type 5070A | Type 1700A111A2 Type 1200A27 | Type 2825A-02 | |

Figure 5. Measuring chain of cutting force used in the experiment [28]

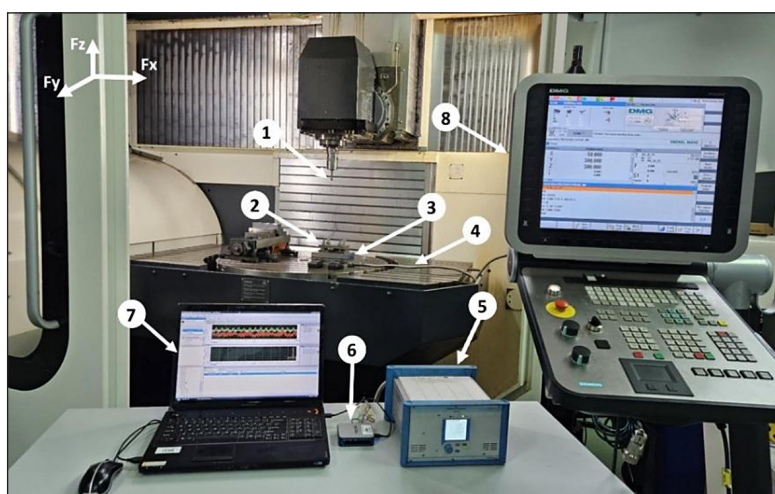


Figure 6. Test stand: 1 – tool, 2 – machine vice, 3 – Kistler 9257B dynamometer, 4 – connection cable, 5 – Kistler 5070A charge amplifier, 6 – DAQ system, 7 – PC with DynoWare, 8 – machine tool control panel

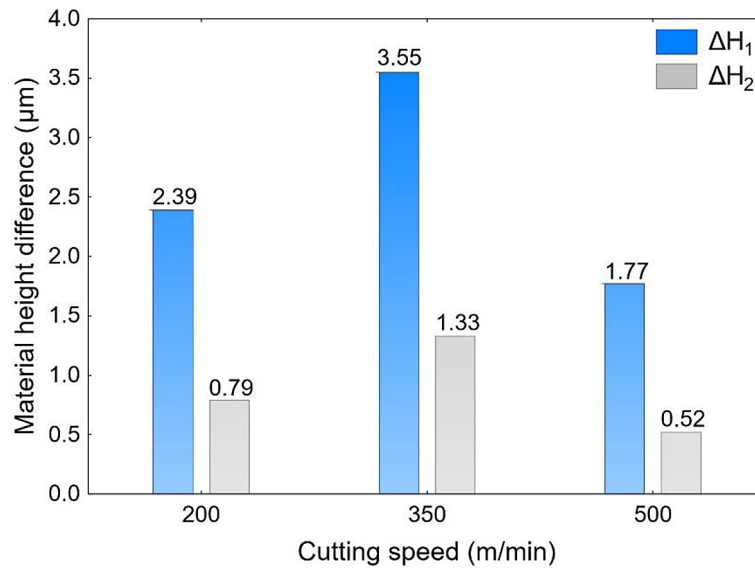


Figure 7. Material height difference after milling with feed rate of 0.04 mm/tooth and using a tool with helix angle of 20°

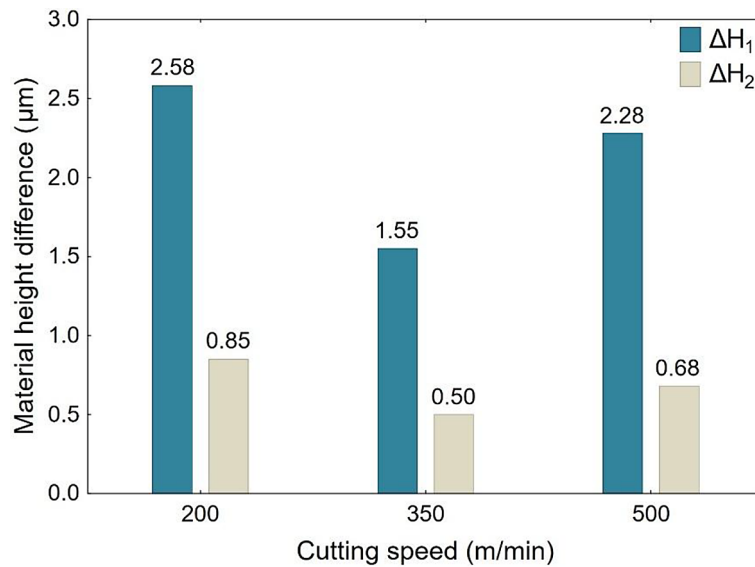


Figure 8. Material height difference after milling with feed rate of 0.06 mm/tooth and using a tool with helix angle of 20°

The milling process with a feed rate of 0.06 mm/tooth and tool with a helix angle of 20° (Figure 8) resulted in the highest material height difference ($\Delta H_1 = 2.58 \mu\text{m}$) for a cutting speed of 200 m/min and the lowest value ($\Delta H_2 = 0.50 \mu\text{m}$) for $v_c = 350 \text{ m/min}$. In this case, as in milling with the lowest value of the f_z parameter, there was an alternating increase and decrease in ΔH_1 and ΔH_2 for the same cutting speeds.

Figure 9 shows values of ΔH_1 and ΔH_2 obtained for the highest value of the feed rate ($f_z = 0.08 \text{ mm/tooth}$) after machining with a milling cutter with a helix angle of 20°. The highest value

of the material height difference ($\Delta H_1 = 5.28 \mu\text{m}$) was obtained when machining with $v_c = 350 \text{ m/min}$. The lowest value ($\Delta H_2 = 0.27 \mu\text{m}$) was observed for $v_c = 500 \text{ m/min}$. The analysed variables followed the same trend as for machining with a feed rate of 0.04 mm/tooth.

Figures 10–12 demonstrate the formation of material height differences after the milling process with variable feed rate and the use of a tool with a helix angle of 35°.

The highest ($\Delta H_1 = 5.29 \mu\text{m}$) and the lowest ($\Delta H_2 = 1.17 \mu\text{m}$) values of the materials height differences during machining using the feed rate

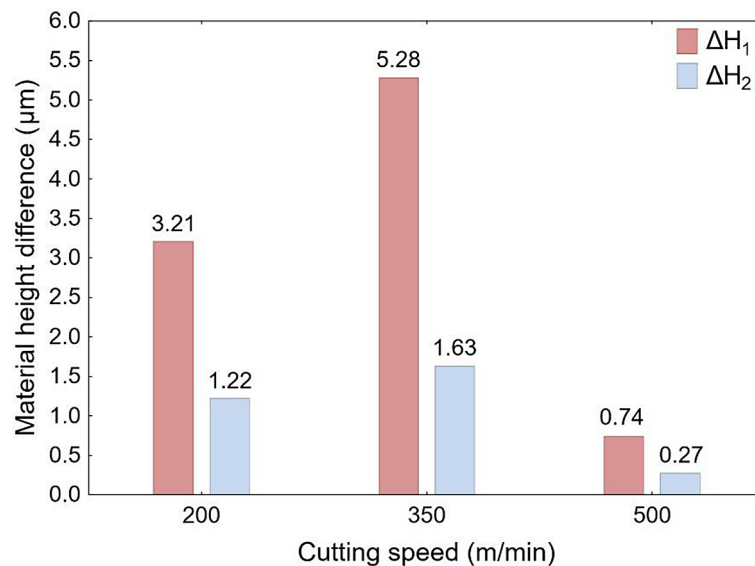


Figure 9. Material height difference after milling with feed rate of 0.08 mm/tooth and using a tool with helix angle of 20°

of 0.04 mm/tooth and a tool with a helix angle of 20° were obtained with the highest value of the cutting speed ($v_c = 500$ m/min). It can be seen that ΔH_1 increases as the cutting speed increases. In the case of the ΔH_2 variable, the values remain at a similar level (from 1.17 μm to 1.45 μm), but it reaches the highest value for $v_c = 350$ m/min (Figure 10). The highest value of the material height difference ($\Delta H_1 = 7.08$ μm) after milling with the f_z parameter of 0.06 mm/tooth was obtained at a cutting speed of 350 m/min, while the lowest value ($\Delta H_2 = 0.79$ μm) was achieved with the highest value of the v_c parameter. It can be seen that,

while no clear trend may be noticed for ΔH_1 , for ΔH_2 , as the cutting speed increased, the quality of the machined surface also increased (values of ΔH_2 decreased).

The milling process with using the f_z parameter of 0.08 mm/tooth resulted in the highest material height difference ($\Delta H_1 = 7.29$ μm) for $v_c = 200$ m/min and the lowest value ($\Delta H_2 = 1.74$ μm) for the cutting speed of 500 m/min. By analysing the data in Figure 12, it can be seen that for both ΔH_1 and ΔH_2 , the material height differences decrease as the cutting speed increases. In each case considered, higher values of ΔH_1 than ΔH_2

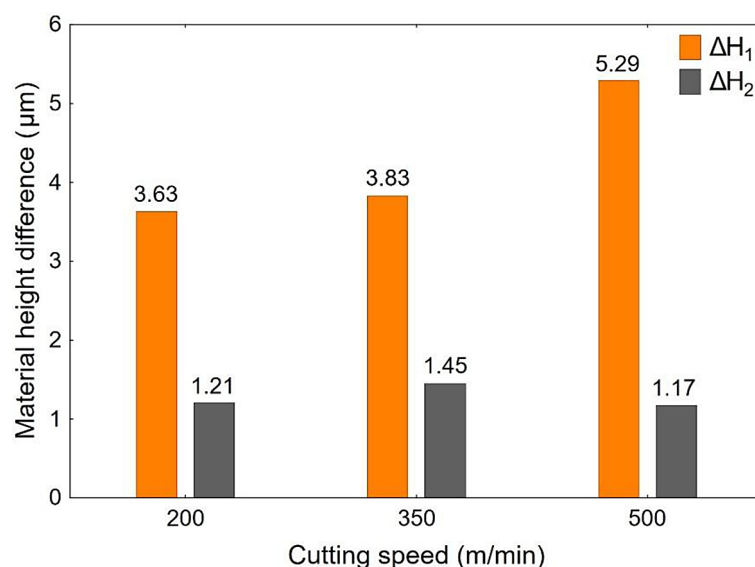


Figure 10. Material height difference after milling with feed rate of 0.04 mm/tooth and using a tool with helix angle of 35°

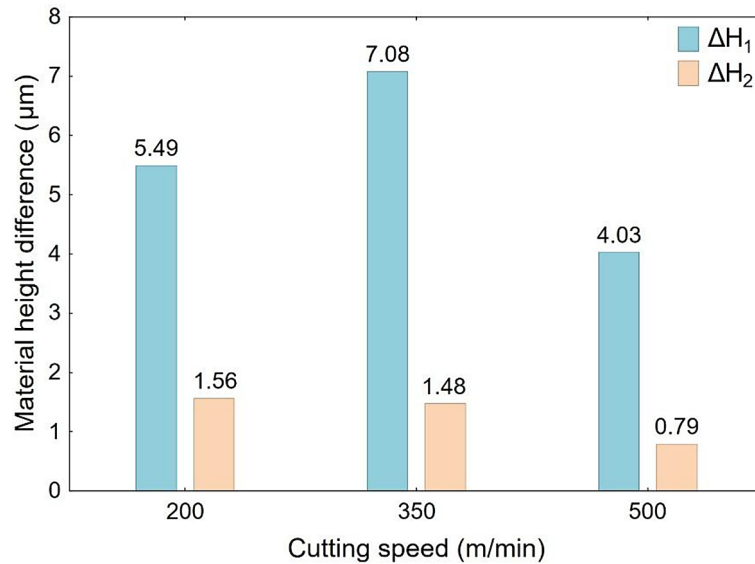


Figure 11. Material height difference after milling with feed rate of 0.06 mm/tooth and using a tool with helix angle of 35°

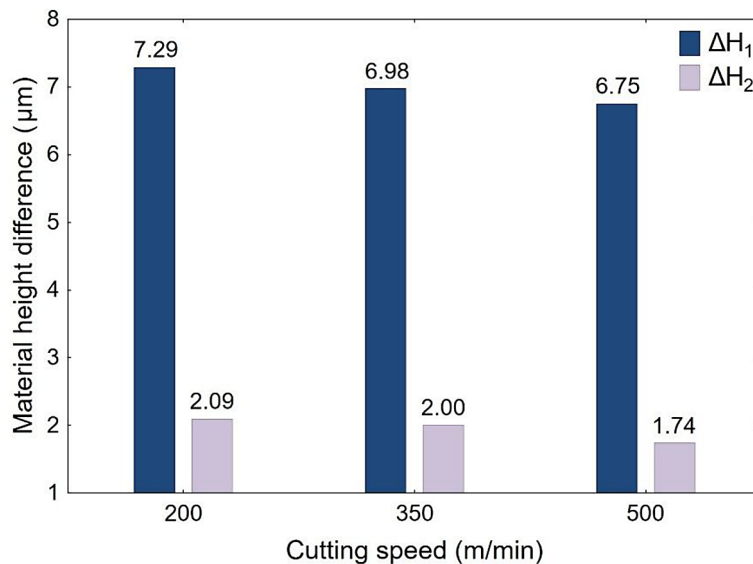


Figure 12. Material height difference after milling with feed rate of 0.08 mm/tooth and using a tool with helix angle of 35°

were obtained. Thus, a higher material height difference occurred when moving from a lower strength material (aluminium alloy) to a higher strength material (CFRP). This may indicate that the lower stiffness material presses against the edge of the higher stiffness material. In addition, the aluminium alloy may have been set back by the cutting edge of the tool and the composite layer [29]. In most cases, poorer surface quality was obtained after machining with a tool with a helix angle of 35°. A higher value for this angle contributes primarily to faster chip removal. On the other hand, it is less rigidity and stability of the

tool, which in the case of machining thin-walled workpieces probably had the greatest influence on the obtained results [30].

When comparing the surface quality after the milling for the same values of the f_z parameter and different tools geometry, it can be seen that for the f_z parameter of 0.04 mm/tooth, the same course of ΔH_1 and ΔH_2 was obtained. Comparing the results of the material height difference for $f_z = 0.06$ mm/tooth, it can be noticed that the type of tool has a different effect on the material height difference. For $f_z = 0.08$ mm/tooth, a different trend of ΔH_1 and ΔH_2 was obtained for analyzed tools.

Furthermore, for a tool with a helix angle of 35° , similar values of ΔH_1 (from $7.29 \mu\text{m}$ to $6.75 \mu\text{m}$) and ΔH_2 (from $2.09 \mu\text{m}$ to $1.75 \mu\text{m}$) were obtained. For a helix angle of 20° , the differences obtained for ΔH_1 (from $5.28 \mu\text{m}$ to $0.74 \mu\text{m}$) and ΔH_2 (from $1.63 \mu\text{m}$ to $0.27 \mu\text{m}$) were much higher.

Feed force

Figures 13 and 14 show the feed force amplitudes recorded during machining with the adopted cutting parameters. Based on Figures 13 and 14 it can be observed that increasing the cutting

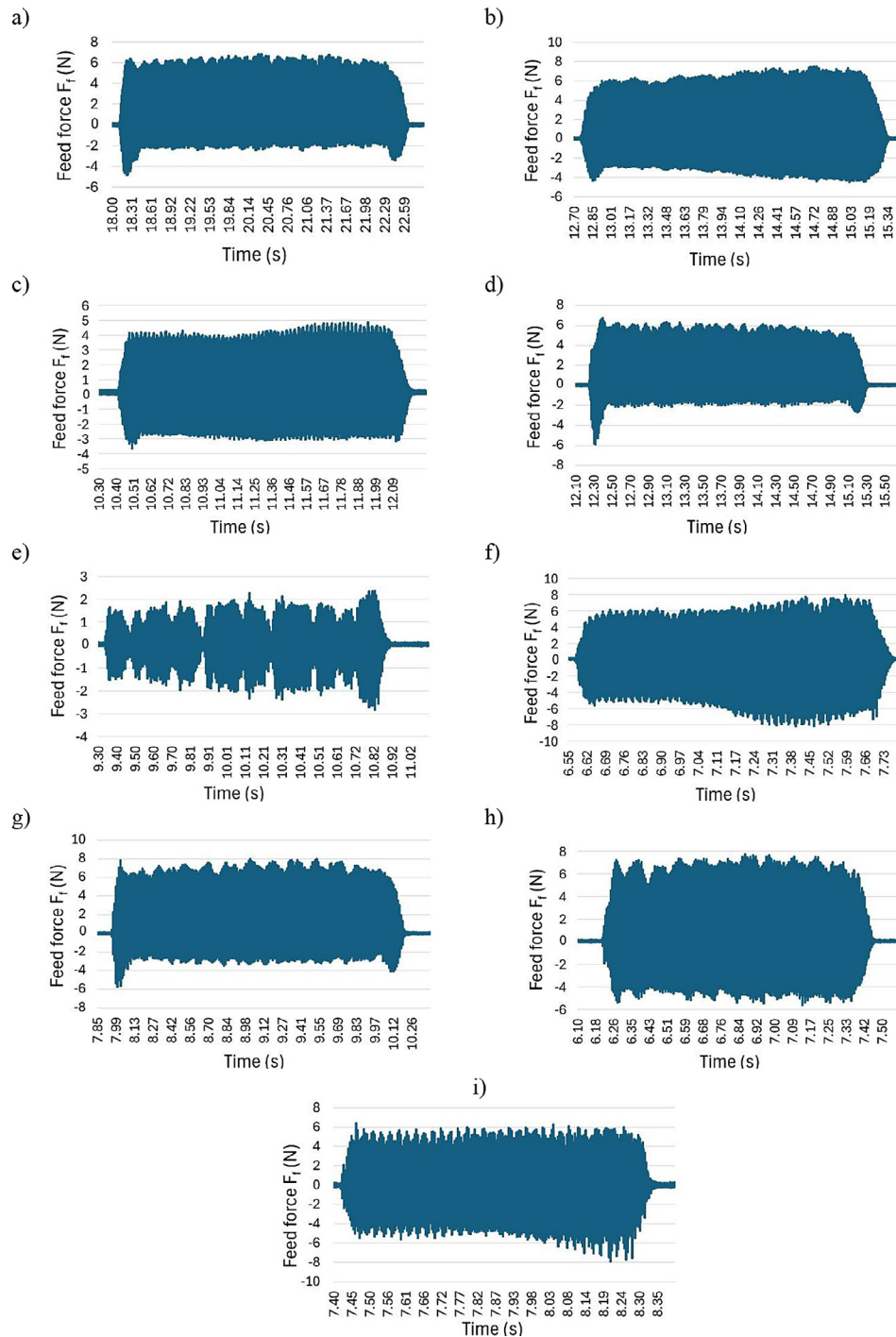


Figure 13. Feed force amplitudes during milling with a tool with helix angle of 20° using cutting parameters:

- (a) $v_c = 200 \text{ m/min}$, $f_z = 0.04 \text{ mm/tooth}$, (b) $v_c = 350 \text{ m/min}$, $f_z = 0.04 \text{ mm/tooth}$, (c) $v_c = 500 \text{ m/min}$, $f_z = 0.04 \text{ mm/tooth}$, (d) $v_c = 200 \text{ m/min}$, $f_z = 0.06 \text{ mm/tooth}$, (e) $v_c = 350 \text{ m/min}$, $f_z = 0.06 \text{ mm/tooth}$, (f) $v_c = 500 \text{ m/min}$, $f_z = 0.06 \text{ mm/tooth}$, (g) $v_c = 200 \text{ m/min}$, $f_z = 0.08 \text{ mm/tooth}$, (h) $v_c = 360 \text{ m/min}$, $f_z = 0.08 \text{ mm/tooth}$, (i) $v_c = 500 \text{ m/min}$, $f_z = 0.08 \text{ mm/tooth}$.

speed tended to result in higher amplitudes in the final machining phase. It can also be concluded that higher values of the v_c parameter resulted in more symmetrical shaped amplitudes, indicating that the cutting forces acting on the tool during machining are uniformly distributed and do not

induce additional torques [31]. Increasing the values of the feed rate did not affect the symmetry of the obtained feed force amplitudes.

Figures 15–17 illustrate the average values of the feed force F_f depending on the adopted machining parameters and cutting tool geometry.

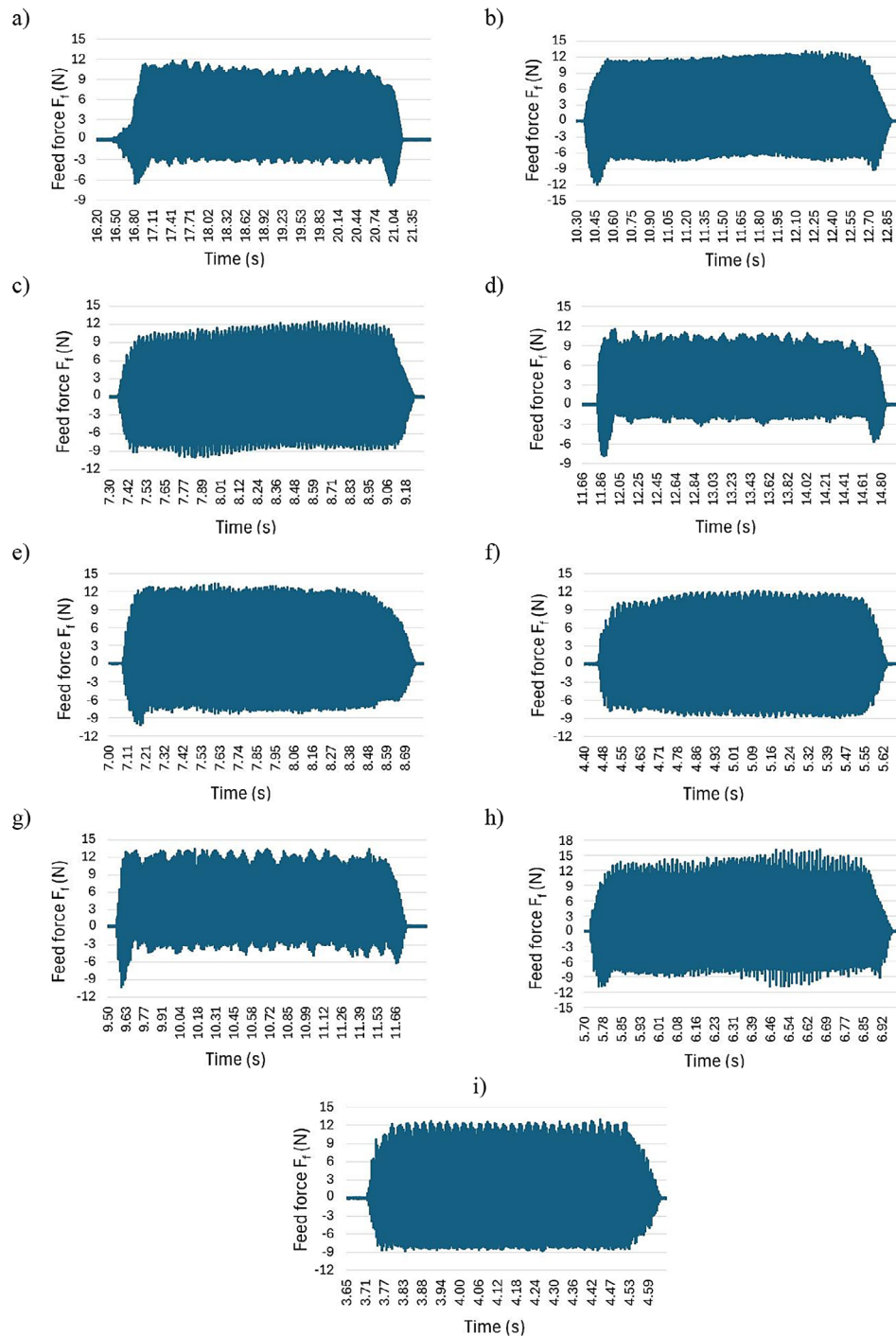


Figure 14. Feed force amplitudes during milling with a tool with helix angle of 35° using cutting parameters:

- (a) $v_c = 200$ m/min, $f_z = 0.04$ mm/tooth, (b) $v_c = 350$ m/min, $f_z = 0.04$ mm/tooth, (c) $v_c = 500$ m/min, $f_z = 0.04$ mm/tooth, (d) $v_c = 200$ m/min, $f_z = 0.06$ mm/tooth, (e) $v_c = 350$ m/min, $f_z = 0.06$ mm/tooth, (f) $v_c = 500$ m/min, $f_z = 0.06$ mm/tooth, (g) $v_c = 200$ m/min, $f_z = 0.08$ mm/tooth, (h) $v_c = 360$ m/min, $f_z = 0.08$ mm/tooth, (i) $v_c = 500$ m/min, $f_z = 0.08$ mm/tooth

For the f_z parameter of 0.04 mm/tooth, the maximum value of the feed force ($F_f = 39.50$ N) was obtained during milling with a tool with a helix angle of 35° and using the highest value of the v_c parameter. The lowest value of the feed force ($F_f = 19.10$ N) in this case was obtained for a milling cutter with a helix angle of 20° and a cutting speed of 350 m/min. Based on the data shown in Figure 15, it can be seen that for both cutting tool geometries, a similar trend of F_f was obtained – there is a noticeable decrease in the feed force as the cutting speed increases from $v_c = 200$ m/min to $v_c = 350$ m/min, followed by an increase for the highest value of this parameter. Increasing the feed rate to a value of 0.06 mm/tooth resulted in

the highest value of feed force ($F_f = 44.40$ N) for a milling cutter with a helix angle of 35° and a v_c parameter of 500 m/min. The lowest value in this case ($F_f = 7.30$ N) was recorded during machining with a tool with a helix angle of 20° and using a v_c parameter of 350 m/min. Analysing the data shown in Figure 16, it can be observed that for a tool with a higher helix angle, the values of feed force F_f increased as the v_c parameter increased. A similar conclusion was reached based on research contained in [32]. A milling cutter with a helix angle of 20° shows a significant decrease in feed force for a cutting speed of 350 m/min, followed by an increase for $v_c = 500$ m/min. This may be related to the delamination of the machined

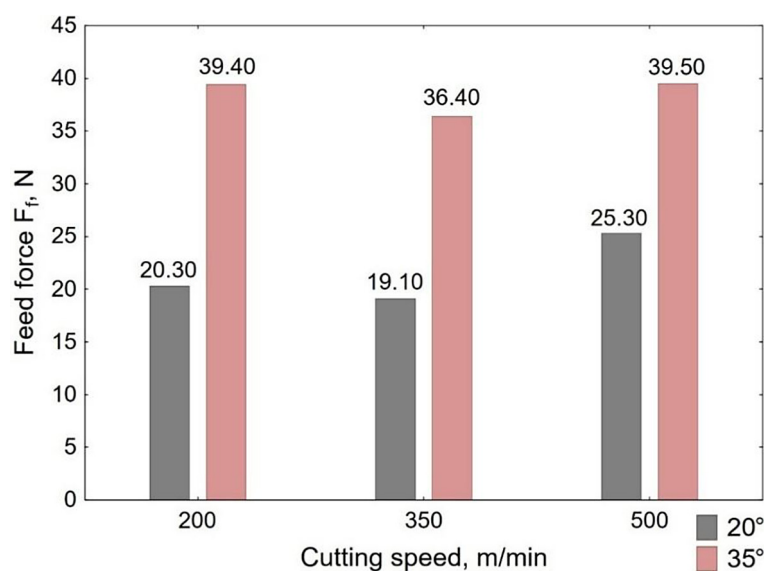


Figure 15. Feed force F_f after machining with feed rate of 0.04 mm/tooth

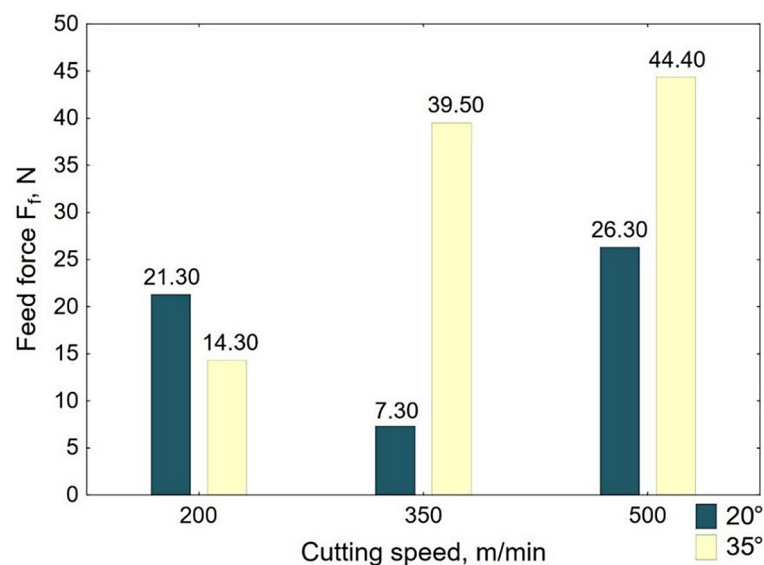


Figure 16. Feed force F_f after machining with feed rate of 0.06 mm/tooth

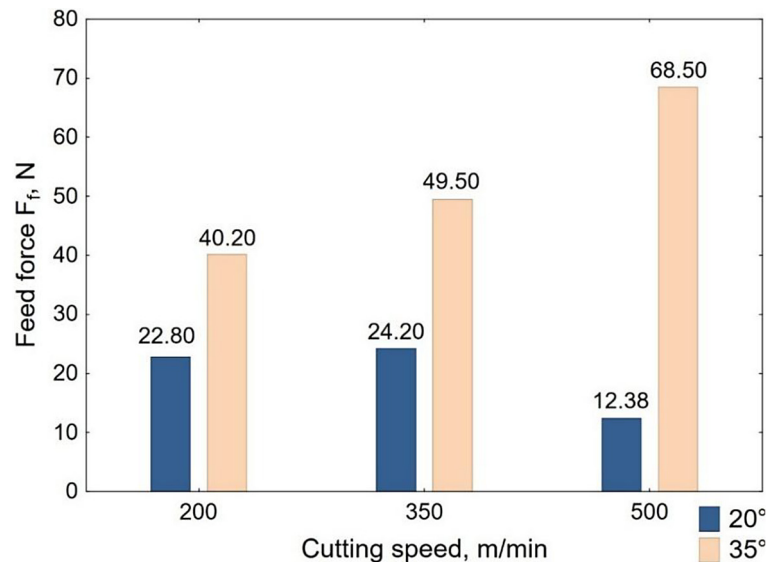


Figure 17. Feed force F_f after machining with feed rate of 0.08 mm/tooth

surface – in Figure 13 e it is possible to find alternating places where the amplitudes reach values of 0. This indicates that there were defects in the machined structure on the surface of the sample, causing a decrease in the average value of the feed force F_f .

Figure 17 illustrates the results of the average value of the feed force F_f recorded during milling using the f_z parameter of 0.08 mm/tooth. The highest value of feed force ($F_f = 68.50$ N) was obtained after milling with a helix angle of 35° and using the highest value of cutting speed. The lowest value of the analysed variable ($F_f = 12.38$ N) was obtained for the same value of the cutting speed, but with a milling cutter with a helix angle of 20° . For a tool with a higher helix angle, it is noticeable that the value of F_f increases with increasing cutting speed. For a tool with a helix angle of 20° , there is no clear effect of the v_c parameter on the analysed variable. By comparing the results shown in Figure 17 and Figure 13 i, it can be concluded that obtaining the lowest F_f value for these machining conditions may also be the result of delamination of the machined surface – the feed force amplitudes decrease in the middle of the tool path and then increase at the tool exit, which may indicate material delamination at the end of the sample.

Comparing the surface quality results and the average values of the cutting force, it can be seen that the highest and lowest values of the material height differences were not achieved for the same cutting parameters as the highest and lowest values of the feed force F_f .

In [29] it was noted that during the face milling of parallel workpieces, machining of higher strength material results in an increase in the feed force F_f , which is reflected in an increase in material height differences. In this experiment, no similar trend was found. This is due to the fact that the feed force F_f was the average value recorded when the tool passed through the entire surface of the sample. In the case of the circumferential milling, it is not possible to isolate a phase in which the tool is machining only one layer of FLM. However, it can be assumed that the higher difference occurring between the feed forces for each material-forming layers, the poorer surface quality of the sample after machining [33].

CONCLUSIONS

The aim of the study was to determine the effects of the cutting speed, feed rate and helix angle on the material height differences and cutting forces after milling of CARALL. The following conclusions were drawn from the study:

1. Poorer surface quality and higher cutting forces were obtained for a tool with a higher helix angle.
2. Higher material height differences were achieved at the metal-composite interface (ΔH_1) than at the composite-metal interface (ΔH_2).
3. The use of higher values of the v_c parameter resulted in more symmetrical and evenly distributed the feed force amplitudes.
4. Increasing the feed rate resulted in increasing the feed force amplitudes at the cutting tool

exit, illustrating the lower stability of machining and the possibility of delamination at the end of the samples.

5. The parameters to obtain the best surface quality (the lowest material height difference) are the cutting speed of 500 m/min, feed rate of 0.08 mm/tooth and helix angle of 20°.
6. The lowest surface accuracy (the highest value of the material height difference) was obtained after milling with the following milling parameters: cutting speed of 200 m/min, feed rate of 0.08 mm/tooth and helix angle of 35°.

Acknowledgments

The research leading to these results has received funding from the commissioned task entitled “VIA CARPATIA Universities of Technology Network named after the President of the Republic of Poland Lech Kaczyński” under the special purpose grant from the Minister of Education and Science, contract no. MEiN/2022/DPI/2575, as part of the action “In the neighborhood - inter-university research internships and study visits.

REFERENCES

1. Alderliesten R. Laminate Concepts & Mechanical Properties. In: Fatigue and Fracture of Fibre Metal Laminates. Solid Mechanics and Its Applications. 2017; 236. Springer, Cham. https://doi.org/10.1007/978-3-319-56227-8_2
2. Chai G.B., Manikandan P. Low velocity impact response of fibre-metal laminates – A review. Compos. Struct. 2014; 107: 363–381. <https://doi.org/10.1016/j.compstruct.2013.08.003>
3. Chen Y., Wang Y., Wang H. Research progress on interlaminar failure behavior of fiber metal laminates. Adv. Polym. Tech. 2020; 2020: 3097839. <https://doi.org/10.1155/2020/3097839>
4. Ebrahimnezhad-Khaljiri H., Eslami-Farsani R., Akbarzadeh E. Effect of interlayer hybridization of carbon, kevlar, and glass fibers with oxidized polyacrylonitrile fibers on the mechanical behaviors of hybrid composites. Proc. Inst. Mech. Eng. Part C. 2020; 234: 1823–1835. <https://doi.org/10.1177/09544062198979>
5. Kazemi M.E., Shanmugam L., Yang L., Yang J. A Review on the hybrid titanium composite laminates (HTCLs) with focuses on surface treatments, fabrications, and mechanical properties. Compos. Part A Appl. Sci. Manuf. 2020; 128: 105679. <https://doi.org/10.1016/j.compositesa.2019.105679>
6. Xie M., Zhan L., Ma B., Hui S. Classification of fiber metal laminates (FMLs), adhesion theories and methods for improving interfacial adhesion: A review. Thin-Walled Struct. 2024; 198: 111744. <https://doi.org/10.1016/j.tws.2024.111744>
7. Kłonica M. Application of the ozonation process for shaping the energy properties of the surface layer of polymer construction materials. J. Ecol. Eng. 2022; 23: 212–219. <https://doi.org/10.12911/22998993/145265>
8. Kłonica M., Matuszak J., Zagórski I. Effect of milling technology on selected surface layer properties. In: 2019 IEEE 5th International Workshop on Metrology for AeroSpace (MetroAeroSpace). IEEE, Torino, Italy, June; 2019. <https://doi.org/10.1109/MetroAeroSpace.2019.8869621>
9. Feito N., Diaz-Alvarez J., Lopez-Puente J., Miguelez M.H. Numerical analysis of the influence of tool wear and special cutting geometry when drilling woven CFRPs. Compos. Struct. 2016; 138: 258–294. <https://doi.org/10.1016/j.compstruct.2015.11.065>
10. Ciecieląg K., Zaleski K., Kęcik K. Effect of milling parameters on the formation of surface defects in polymer composites. Mater. Sci. 2022; 57: 882–893. <https://doi.org/10.1007/s11003-022-00622-w>
11. Doluk E., Rudawska A., Miturska-Barańska I. Investigation of the surface roughness and surface uniformity of a hybrid sandwich structure after machining. Materials 2022; 15: 7299. <https://doi.org/10.3390/ma15207299>
12. Costa R.D.F.S., Sales-Contini R.C.M., Silva F.J.G., Sebbe N., Jesus A.M.P. A. Critical review on fiber metal laminates (FML): From manufacturing to sustainable processing. Metals 2023; 13: 638. <https://doi.org/10.3390/met13040638>
13. Ekici E., Motorcu A.R., Yildirim E. An experimental study on hole quality and different delamination approaches in the drilling of CARALL, a new FML composite. FME Transaction 2021; 49: 950–961. <https://doi.org/10.5937/fme2104950E>
14. Mani N., Subbiah D., Moorthy A., Arunagiri A. Optimization and prediction of machining parameters in nanoparticle-reinforced FMLs using AI techniques. Rev. Matér. 2025; 30: 1–15. <https://doi.org/10.1590/1517-7076-RMAT-2024-0645>
15. Sourd X., Giasin K., Zitoun R., Salem M., Lupton C. Multi-scale analysis of the damage and contamination in abrasive water jet drilling of GLARE fibre metal laminates. J. Manuf. Process. 2022; 84: 610–621. <https://doi.org/10.1016/j.jmapro.2022.10.023>
16. Logesh K., Moshi A.A.M., Bharathi S.R.S., Hariharasakthisudhan P. A multi-objective grey relational approach and regression analysis on optimization of drilling process parameters for glare fiber metal laminates. Surf. Rev. and Lett. 2022; 29: 2250066. <https://doi.org/10.1142/S0218625X22500664>

17. Liu Ch.H., Wang Ch.Ch., Lai W.M. Shen M.Y. Optimization of machining quality for carbon fiber reinforced thermoplastic polymer/aluminum hybrid laminates via ultrasonic-assisted processing and interfacial modification. *Compos. B: Eng.* 2025; 300: 112498. <https://doi.org/10.1016/j.compositesb.2025.112498>
18. Doluk E. Comparison of hole quality after drilling and helical milling of the Al/CFRP stacks. *TiAM.* 2023; 122: 3–12. <https://doi.org/10.7862/tiam.2023.4.1>
19. Bolar G., Sridhar A.K., Ranjan A. Drilling and helical milling for hole making in multi-material carbon reinforced aluminum laminates. *Int. J. Lightweight Mater. Manuf.* 2022; 5: 113–125. <https://doi.org/10.1016/j.ijlmm.2021.11.004>
20. Wang H., Qin X., Li H., Tan Y. A comparative study on helical milling of CFRP/Ti stacks and its individual layers. *Int. J. Adv. Manuf. Technol.* 2016; 86: 1973–1983. <https://doi.org/10.1007/s00170-015-8296-3>
21. Xiao H., Sultan M.T.H., Shahar F.S., Gaff H.D. Recent developments in the mechanical properties of hybrid fiber metal laminates in the automotive industry: A review. *Rev. Adv. Mater. Sci.* 2023; 62: 20220328. <https://doi.org/10.1515/rams-2022-0328>
22. Ma Q., Merzuki M.N.M., Rejab M.R.M., Sani M.S.M., Zhang B. A review of the dynamic analysis and free vibration analysis on fiber metal laminates (FMLs). *Funct. Compos. Struct.* 2023; 5: 012003. <https://doi.org/10.1088/2631-6331/acb135>
23. Murni A., Abdullah A.S. A review on mechanical properties and response of fibre metal laminate under impact loading (Experiment). *EVERGREEN Joint Journal of Novel Carbon Resource Sciences & Green Asia Strategy.* 2023; 10: 111–129. <https://doi.org/10.5109/6781057>
24. Gülcan O., Tekkanat K., Çetinkaya B. A review on fiber metal laminates and their usage in aerospace industry. *Engineer and Machinery* 2019; 60: 262–288. <https://doi.org/10.46399/muhendismakina.677991>
25. EN 573-3+A2:2024-06 – Aluminium and aluminium alloys – Chemical composition and form of wrought products – Part 3: Chemical composition and form of products.
26. EN 485-2+A1:2018-12 – Aluminium and aluminium alloys – Sheet, strip and plate – Part 2: Mechanical properties.
27. Hoffmann Group. Catalogue 1 Machining/Clamping Technology; Hoffmann Group: Munich, Germany, 2019.
28. Kistler Group. Product Catalogue Sensors and Solutions for Cutting Force Measurement; Kistler Group: Winterthur, Switzerland, 2015.
29. Denkena B., Köhler J., Hasselberg E. Modeling of workpiece shape deviations in face milling of parallel workpiece compounds. *Proc. CIRP.* 2013; 8: 176–181. <https://doi.org/10.1016/j.procir.2013.06.085>
30. Płodzień M., Burek J., Żyłka Ł., Sułkiewicz P. The influence of end mill helix angle on high performance milling process. The influence of end mill helix angle on high performance milling process. *JMST.* 2020; 34: 817–827. <http://doi.org/10.1007/s12206-020-0131-6>
31. Meng B., Liu X., Li M., Liang S.Y., Wang L., Wang Z. Uniformity, periodicity and symmetry characteristics of forces fluctuation in helical-edge milling cutter. *Appl. Sci.* 2021; 11: 2693. <https://doi.org/10.3390/app11062693>
32. Ciecieląg K. Evaluation of machinability indicators in milling of thin-walled composite structures. *Adv. Sci. Technol. Res. J.* 2024; 18: 202–212. <https://doi.org/10.12913/22998624/177362>
33. Denkena B., Grove T., Hasselberg E. Workpiece shape deviations in face milling of hybrid structures. *MSF.* 2015; 825–826: 336–343. <https://doi.org/10.4028/www.scientific.net/msf.825-826.336>